Present-day kinematics at the India-Asia collision zone

Brendan J. Meade
Department of Earth and Planetary Sciences, Harvard University, 20 Oxford Street, Cambridge, Massachusetts 02138, USA

ABSTRACT

The collision of the Indian subcontinent with Asia drives the growth and evolution of the greater Tibetan Plateau region. Fault slip rates resulting from the relative motion between crustal blocks can provide a kinematic description of the distribution of present-day deformation. I construct a three-dimensional, regional-scale elastic block model of the India-Asia collision zone that is consistent with geodetic observations of interseismic deformation, mapped fault system geometry, historical seismicity, and the mechanics of the earthquake cycle. This mechanical model of the elastic upper crust yields a set of kinematically consistent fault slip rates and block motions that may serve to constrain dynamic models of continental crustal dynamics.

Keywords: India-Asia collision, faulting, geodetic velocities, upper crust.

INTRODUCTION

The Indian subcontinent has been colliding with Eurasia for ~50 m.y., leading to the emergence and growth of the Tibetan Plateau. Although large-scale structures at the collision zone have been recognized for several decades (Molnar and Tapponnier, 1975), the mechanics governing the present-day behavior and historical evolution of the greater Tibetan Plateau region have been debated. Dynamic models of a thin viscous sheet representing the lithosphere have accounted for the critical features of the collision zone, including its great elevation and the lateral spreading of the Tibetan Plateau (England and Houseman, 1989; England and Molnar, 1997). However, these regional-scale models do not represent the mechanical behavior of the seismogenic upper crust, for which there are direct measurements of fault slip and interseismic displacement rates. While geodetically determined surface velocities have been interpreted in the context of viscous sheet models (England and Molnar, 2005), the behavior of an elastic upper layer has been neglected at large spatial scales. If the lithosphere is modeled as an elastic layer over a viscous (or viscoelastic) sublayer, then steady-state surface velocities provide no diagnostic information about the distribution of viscous deformation throughout lithosphere below the elastic layer (Hetland and Hager, 2004; Savage, 2000; Zatman, 2000). Instead, geodetically measured interseismic surface velocities largely contain information about the motion of crustal blocks and elastic strain accumulation surrounding faults in the upper crust, but not the long-term behavior of the bulk lithosphere. Thus, models constrained by interseismic geodetic observations require an explicit treatment of the upper crust and, in particular, the mechanics of the earthquake cycle.

Geodetic displacement rates and two-dimensional models of the earthquake cycle (Savage and Burford, 1973) have been used to estimate the motion of individual faults, including the Altyn Tagh at the northern edge of the Tibetan Plateau (Bendick et al., 2000; Wright et al., 2004). These studies have found ~7 ± 3 mm/yr slip rates that are ~30%–50% lower than those inferred from offset geologic features that postdate the Last Glacial Maximum (Meriaux et al., 2005; Tapponnier et al., 2001). These relatively low geodetically constrained slip rate estimates combined with the gradients in the regional velocity fields (Wang et al., 2001; Zhang et al., 2004) have been used to suggest that the tectonics of the greater Tibetan Plateau region are best described as continuous, and that global position system (GPS) observations cannot be explained in terms of the motion of crustal blocks and elastic strain accumulation (Jade et al., 2004; Zhang et al., 2004).

BLOCK MODEL

The purpose of this paper is to integrate geodetic and geologic observations into an internally consistent, three-dimensional, regional-scale model in order to image the elastic behavior of the elastic upper crust and to test the hypothesis that deformation at the India-Asia collision zone can be represented accurately by block tectonics. To describe the recent behavior of the India-Asia collision zone I develop an elastic block model that allows us to invert geodetically constrained surface velocities for a set of kinematically consistent slip rates on major faults while simultaneously accounting for the effects of block rotations and interseismic elastic strain accumulation (Meade and Hager, 2005). The predicted interseismic velocity at a point is equal to the sum of the block velocity and the integrated effects of elastic strain accumulation from all faults. The locking of the upper seismogenic part of the fault zone during the interseismic phase of the seismic cycle gives rise to elastic strain accumulation effects that cause across-fault velocity gradients to be smooth, rather than stepped as they are over geologic time. Thus, we assume that GPS velocities are representative of crustal deformation over earthquake cycle time scales (hundreds of years) but not longer-term geologic time scales (>10 k.y.). We also assume that GPS velocities throughout the interseismic part of the seismic cycle are approximately time invariant, consistent with a relatively high viscosity (>10^{19} Pa·s) for the lower crust–upper mantle (e.g., Savage, 2000).

The block model geometry is based on published fault maps (Kapp and Guynn, 2004; Peltzer and Saucier, 1996; Tapponnier et al., 2001) (see GSA Data Repository[1]) and consists of 17 blocks ranging in size from plate scale to 10,000 km^2 for the smallest blocks at the eastern edge of the plateau (Figs. 1 and 2). The block boundaries are correlated with the locations of major faults that are assumed to be vertical, with the exception of the Himalayan thrust system, which dips ~10° northward. Some block boundaries, especially those in southeast Asia, are speculative because they improve the fit to the data yet do not correlate with any mapped structure of which I am aware. In this sense, the geodetic data and block model can be considered a tool to identify possible shear zones and incorporate mapped fault system geometry. The most notable of these

[1]GSA Data Repository item 2007025, Table DR1 and Figures DR1–DR3 (fault geometry, block boundaries, residual velocities, and moment rates), is available online at www.geosociety.org/pubs/ft2007.htm, or on request from editing@geosociety.org or Documents Secretary, GSA, P.O. Box 9140, Boulder, CO 80301, USA.

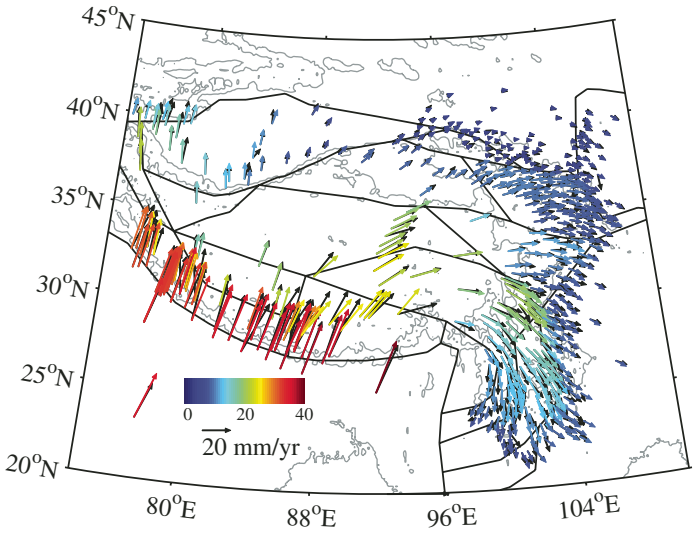

Figure 1. Observed and modeled velocities in Eurasian reference frame. Observed velocities (black arrows) are overlain by model velocities, which are colored by magnitude. Reddish colors indicate larger magnitudes. Thin gray lines are 2000 m elevation contours and thick black lines are block model boundaries. Both sets of velocities show north-south convergence across western half of Tibetan Plateau and transport of material toward southeastern Asia.

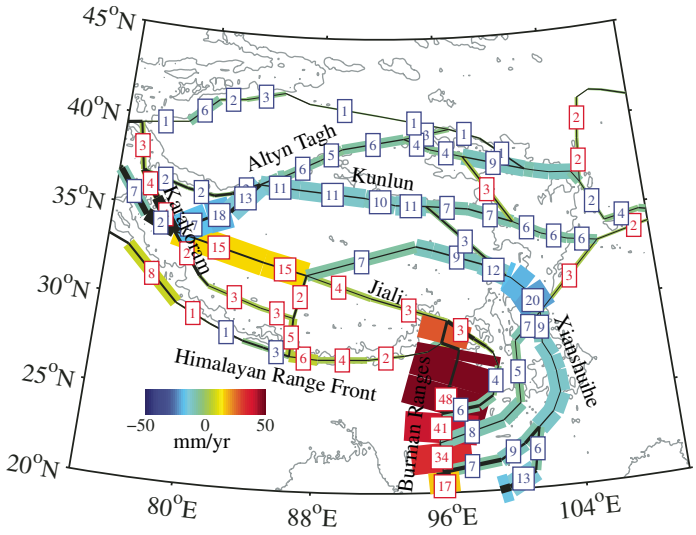

Figure 2. Model strike-slip rates (rounded to nearest whole number). Red and blue shades indicate right- and left-lateral slip, respectively. Wider lines indicate higher slip magnitudes. Black lines are slip rate uncertainties. Strike-slip motion on east-west–trending faults accommodates eastward motion of material from Tibetan Plateau toward southeast Asia.

speculative boundaries within the plateau is the northwest- to southeast-striking boundary extending from the Quilanshan to the eastern Kunlun fault that improves the goodness of fit of the east velocity components. An additional assumption is that there is a coherent structure between the Jiali and Xianshuihe faults in central Tibet. Compiled fault maps suggest southwest- to northeast-trending structures along this block boundary for at least 50% of its length, though there are multiple candidate faults that may also play an important role (Figure DR1; see footnote 1). If this feature and the eastern Xianshuihe fault are eliminated, the residual velocities increase (most notably the north component) not only locally, but also near the intersection with the inactive Red River fault. In this sense, the geodetic data and block model can be seen as a tool to identify possibly shear zones. The dense geodetic data just to the east of this region were used to identify the Songpan-Xihe deformation zone ~100 km northwest of the Longmenshan (Shen et al., 2005).

Block motions and fault slip rates are constrained by an overdetermined uncertainty weighted least squares estimator using 554 geodetically determined interseismic velocities from northern India to the Tarim basin (Zhang et al., 2004) (Fig. 1). The model and observed velocities agree well with a mean residual (observed and modeled) velocity component magnitude of 1.46 mm/yr compared to the 1.33 mm/yr for the mean velocity uncertainty, and a minimum reduction in variance of 96%. The agreement between the modeled and observed velocities demonstrates that the quasi-static elastic model used is capable of accurately modeling interseismic GPS measurements. This is consistent with the assumption of a high-viscosity lower crust–upper mantle ($\eta > 10^{19}$ Pa·s) and the observed localized velocity gradients near faults, and consistent with two-dimensional models of the Kunlun fault (e.g., Hilley et al., 2005). However, predicted model velocities reproduce the first-order features of the observed velocity field, including both the distribution of north-south shortening and the rotation of material through southeast Asia (Fig. 1). First-order features of the velocity field are recovered, including deformation around the Sichuan Basin and the reorientation of velocities from east-west to north-south trending in southeast Asia. Shen et al. (2005) and Thatcher (2006) estimated similar kinematic behavior for the eastern borderland and the high plateau, focusing on the behavior of GPS stations that were not thought to be affected by elastic strain accumulation.

Due to the fact that slip rates are linear functions of the relative block motions, the slip rates predicted by the block model are internally consistent in the sense that any closed path integral of velocity sums to zero. Estimated fault slip rate uncertainties are functions of the estimated GPS uncertainties, station distribution, and block model geometry, and range from <1 mm/yr for most faults to >7 mm/yr for the faults near the Pamirs, where geodetic coverage is sparse (Figs. 2 and 3). Similar to previous studies (Bendick et al., 2000; Wright et al., 2004), I find left-lateral slip on the Altyn Tagh fault ranging from 2.3 ± 1.3 to 7.2 ± 0.6 mm/yr; the lowest values are at the western end and the fastest rates are east of the intersection with the Kunlun fault (Fig. 2). The slip rate estimate for the Altyn Tagh fault is 2–5 times lower than the 17.8 ± 3.6 mm/yr geologic estimate over the Holocene (Meriaux et al., 2005). Thus, it does not seem that three-dimensional fault system geometry and block rotations can resolve this apparent discrepancy. There is sparse geodetic coverage between the Tibetan Plateau and the Hindu Kush; however, the data suggest that the Karakoram fault slip rate decreases slightly from ~4 to ~2 mm/yr toward the southeast with 1σ uncertainties ranging from 1.5 to 3.7 mm/yr. Within the plateau interior the eastern segment of the Jiali fault slips right laterally at 3.7 ± 0.6 mm/yr (approaching 15 mm/yr at the western end) and both the Kunlun and Xianshuihe faults slip left laterally at ~10 mm/yr. This combination of 5–10 mm/yr of right- and left-lateral strike-slip motion accommodates the eastward motion of the Qiangtang block and demonstrates that deformation is not localized along the faults bounding the Tibetan Plateau. The relative deformation between India and southeast Asia is parameterized as slip on four major faults, the Burman ranges and southern extension of the Xianshuihe fault accommodating ~40 and ~11 mm/yr of right- and left-lateral motion, respectively. At 25°N latitude, this set of faults accommodates ~10 mm/yr of east-west opening (Fig. 3). The south-central plateau also accommodates ~10 mm/yr of east-west extension, consistent with geological observations of ongoing extension since the mid-Miocene (Blisniuk et al., 2001). In agreement with previous local-scale geodetic studies (Bilham et al., 1997; Chen et al., 2004), north-south shortening is largely accommodated by ~20 mm/yr of thrusting

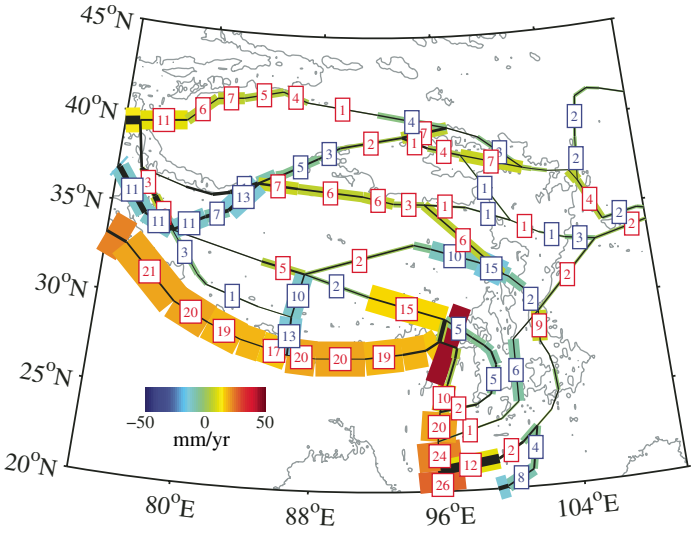

Figure 3. Model tensile and dip-slip rates (rounded to nearest whole number). Reddish and bluish colors indicate convergence and extension, respectively. With the exception of faults along Himalayan range front, all faults are vertical and slip rates are tensile. Highest dip-slip rates are located along Himalayan arc. North-south–trending faults near central Tibetan Plateau show east-west extension.

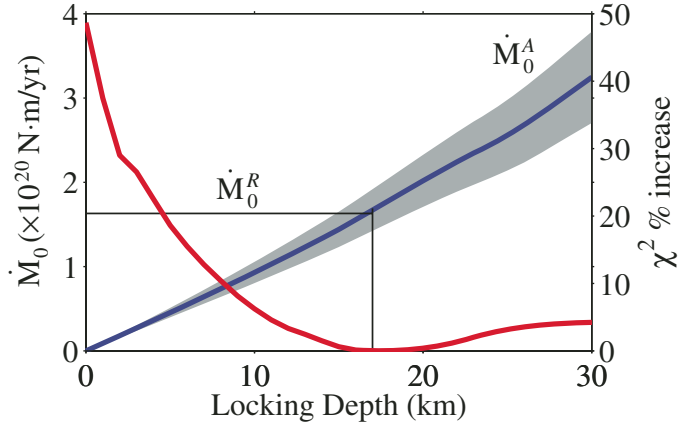

Figure 4. Model moment accumulation rate and goodness of fit as a function of locking depth. Percent increase in velocity misfit, $\chi^2 = \mathbf{r}^T\mathbf{C}^{-1}\mathbf{r}$ ($\mathbf{r}$ is vector of residual velocities, and $\mathbf{C}$ is data covariance matrix), relative to best-fitting model is shown by red line. Model moment accumulation rates, $\dot{M}_0^A$, are shown as blue line, and gray shaded regions show uncertainty range. Thin black horizontal line is historical moment release rate ($\dot{M}_0^R$ = 1.65 × 10²⁰ N·m/yr) and vertical black line connects best-fitting fault locking depth (17 km) to moment accumulation rate at that same depth ($\dot{M}_0^A$ = 1.69 × 10²⁰ N·m/yr).

along the Himalayan range front (HRF) with slip rates decreasing eastward from 24 to 16 mm/yr (Fig. 3). Similarly, clockwise rotation of the Tarim basin (clockwise rotation at 0.55° ± 0.02°/m.y. about an Euler pole located at 90° ± 4° east longitude and 40°1′ ± 2°3′ north latitude) yields ~11 mm/yr of shortening across the central Tien Shan with slip rates decreasing to negligible magnitudes by longitude 95°E, in agreement with integrated models of long-term crustal deformation (Avouac and Tapponnier, 1993) and recent geodetic measurements (Abdrakhmatov et al., 1996). The ~10 mm/yr of shortening across the eastern Jiali fault is inconsistent with the motion of station GNGB to the east of Lhasa. An alternative representation of the fault system near the eastern syntaxis may be required.

The block model slip rate estimates can also be used to make predictions about seismic activity that can be compared with results from studies of recent large Tibetan earthquakes and the record of historical seismicity. Radar measurements of deformation resulting from the 1999 Manyi (M_W = 7.6) earthquake and far-field seismic radiation from the 2001 Kokoxili (M_W = 7.8) earthquake provide evidence of coseismic slip occurring down to a depth of 15–20 km (Antolik et al., 2004; Peltzer et al., 1999). While the locking depths of individual faults are only weakly constrained due to the spacing of geodetic measurements, the reported coseismic rupture depths agree well with the 17 km optimal regional locking depth found using a systematic search of locking depth parameter space (Fig. 4). The historical record of seismicity over the past century provides a synoptic parameterization of coseismic behavior of the fault system in the form of the mean annual rate of moment release, $\dot{M}_0^R$. Updating an existing compilation of moment release from historical earthquakes from 1902 to 1999 (Holt et al., 2000) through 2005, using earthquakes from the Harvard centroid moment tensor catalog, gives a mean annual moment release rate of 1.65 × 10²⁰ N·m/yr for the greater Tibetan Plateau region (78°–110° east longitude, 20°–45° north latitude). If all interseismic elastic strain accumulation is balanced by coseismic strain release, then the present-day moment accumulation rate should balance the historical moment release rate, assuming that the historical earthquake catalog is representative of the typical fault system behavior. The moment accumulation rate for a given fault is the product of shear modulus, fault area, and slip rate magnitude, $\dot{M}_0^A = A\|\dot{\mathbf{s}}\|$. Using a shear modulus of μ = 30 GPa and an optimal locking depth of 17 km, the block model predicts a moment accumulation rate of 1.69 ± 0.24 × 10²⁰ N·m/yr, in good agreement with the moment release rate from the historical earthquake catalog (Fig. 4). The two scalar moment rates deviate by just over ~4%, $\dot{M}_0^A / \dot{M}_0^R \cong 1.04$, indicating that the fault system geometry and predicted slip rates are consistent with the mean seismic behavior over the past century. Shortening along the HRF is responsible for ~35% of the total moment accumulation rate, suggesting that while there may be moment balance over the larger region, there is a localized moment deficit along the HRF, as has been noted (Bilham et al., 2001).

CONCLUSIONS

The three-dimensional elastic block model of the greater Tibetan Plateau region is consistent with the geometry of much of the mapped fault system, geodetic measurements of interseismic deformation, a simple mechanical model of the earthquake cycle, and the historical rate of moment release. The goodness of fit between the model and observed velocities suggests that the high-viscosity approximation of the lower crust–upper mantle may be appropriate within the limit of the assumed Maxwell rheology. Future studies of transient geodetic signals (e.g., postseismic deformation) may help to define the rheology of the subcrustal lithosphere and contribute to the development of vertically integrated and mechanically consistent models for the dynamics of the lithosphere at the India-Asia collision zone.

ACKNOWLEDGMENTS

Rebecca Bendick, Roland Bürgmann, Jeff Freymueller, and four anonymous reviewers of this manuscript and previous drafts provided thoughtful comments that led to a much improved paper.

REFERENCES CITED

Abdrakhmatov, K.Y., Aldazhanov, S.A., Hager, B.H., Hamburger, M.W., Herring, T.A., Kalabaev, K.B., Makarov, V.I., Molnar, P., Panasyuk, S.V., Prilepin, M.T., Reilinger, R.E., Sadybakasov, I.S., Souter, B.J., Trapeznikov, Y.A., Tsurkov, V.Y., and Zubovich, A.V., 1996, Relatively recent construction of the Tien Shan inferred from GPS measurements of present-day crustal deformation rates: Nature, v. 384, p. 450–453, doi: 10.1038/384450a0.

Antolik, M., Abercrombie, R.E., and Ekstrom, G., 2004, The 14 November 2001 Kokoxili (Kunlunshan), Tibet, earthquake: Rupture transfer through a large extensional step-over: Seismological Society of America Bulletin, v. 94, p. 1173–1194, doi: 10.1785/012003180.

Avouac, J.P., and Tapponnier, P., 1993, Kinematic model of active deformation in Central Asia: Geophysical Research Letters, v. 20, p. 895–898.

Bendick, R., Bilham, R., Freymueller, J., Larson, K., and Yin, G.H., 2000, Geodetic evidence for a low slip rate in the Altyn Tagh fault system: Nature, v. 404, p. 69–72, doi: 10.1038/35003555.

Bilham, R., and 24 others, 1997, Nepal Himalaya: Nature, v. 386, p. 61–64, doi: 10.1038/386061a0.

Bilham, R., Gaur, V.K., and Molnar, P., 2001, Himalayan seismic hazard: Science, v. 293, p. 1442–1444, doi: 10.1126/science.1062584.

Blisniuk, P.M., Hacker, B.R., Glodny, J., Ratschbacher, L., Bi, S.W., Wu, Z.H., McWilliams, M.O., and Calvert, A., 2001, Normal faulting in central Tibet since at least 13.5 Myr ago: Nature, v. 412, p. 628–632, doi: 10.1038/35088045.

Chen, Q.Z., Freymueller, J.T., Yang, Z.Q., Xu, C.J., Jiang, W.P., Wang, Q., and Liu, J.N., 2004, Spatially variable extension in southern Tibet based on GPS measurements: Journal of Geophysical Research-Solid Earth, v. 109, doi: 10.1029/2002JB002350.

England, P., and Houseman, G., 1989, Extension during continental convergence, with application to the Tibetan Plateau: Journal of Geophysical Research-Solid Earth, v. 94, p. 17,561–17,579.

England, P., and Molnar, P., 1997, Active deformation of Asia: From kinematics to dynamics: Science, v. 278, p. 647–650, doi: 10.1126/science.278.5338.647.

England, P., and Molnar, P., 2005, Late Quaternary to decadal velocity fields in Asia: Journal of Geophysical Research-Solid Earth, v. 110, doi: 10.1029/2004JB003541.

Hetland, E.A., and Hager, B.H., 2004, Relationship of geodetic velocities to velocities in the mantle: Geophysical Research Letters, v. 31, doi: 10.1029/2004GL020691.

Hilley, G.E., Burgmann, R., Zhang, P.-Z., and Molnar, P., 2005, Bayesian inference of plastosphere viscosities near the Kunlun Fault, northern Tibet: Geophysical Research Letters, v. 32, p. L01302, doi: 10.1029/2004GL021658.

Holt, W.E., Chamot-Rooke, N., Le Pichon, X., Haines, A.J., Shen-Tu, B., and Ren, J., 2000, Velocity field in Asia inferred from Quaternary fault slip rates and Global Positioning System observations: Journal of Geophysical Research-Solid Earth, v. 105, p. 19,185–19,209, doi: 10.1029/2000JB900045.

Jade, S., Bhatt, B.C., Yang, Z., Bendick, R., Gaur, V.K., Molnar, P., Anand, M.B., and Kumar, D., 2004, GPS measurements from the Ladakh Himalaya, India: Preliminary tests of plate-like or continuous deformation in Tibet: Geological Society of America Bulletin, v. 116, p. 1385–1391, doi: 10.1130/B25357.1.

Kapp, P., and Guynn, J.H., 2004, Indian punch rifts Tibet: Geology, v. 32, p. 993–996, doi: 10.1130/G20689.1.

Meade, B.J., and Hager, B.H., 2005, Block models of crustal motion in southern California constrained by GPS measurements: Journal of Geophysical Research-Solid Earth, v. 110, doi: 10.1029/2004JB003209.

Meriaux, A.S., Tapponnier, P., Ryerson, F.J., Xu, X.W., King, G., Van der Woerd, J., Finkel, R.C., Li, H.B., Caffee, M.W., Xu, Z.Q., and Chen, W.B., 2005, The Aksay segment of the northern Altyn Tagh fault: Tectonic geomorphology, landscape evolution, and Holocene slip rate: Journal of Geophysical Research-Solid Earth, v. 110, doi: 10.1029/2004JB003210.

Molnar, P., and Tapponnier, P., 1975, Cenozoic tectonics of Asia—Effects of a continental collision: Science, v. 189, p. 419–426.

Peltzer, G., and Saucier, F., 1996, Present-day kinematics of Asia derived from geologic fault rates: Journal of Geophysical Research-Solid Earth, v. 101, p. 27,943–27,956, doi: 10.1029/96JB02698.

Peltzer, G., Crampe, F., and King, G., 1999, Evidence of nonlinear elasticity of the crust from the Mw7.6 Manyi (Tibet) earthquake: Science, v. 286, p. 272–276, doi: 10.1126/science.286.5438.272.

Savage, J.C., 2000, Viscoelastic-coupling model for the earthquake cycle driven from below: Journal of Geophysical Research-Solid Earth, v. 105, p. 25,525–25,532, doi: 10.1029/2000JB900276.

Savage, J.C., and Burford, R.O., 1973, Geodetic determination of relative plate motion in central California: Journal of Geophysical Research, v. 78, p. 832–845.

Shen, Z.K., Lu, J.N., Wang, M., and Burgmann, R., 2005, Contemporary crustal deformation around the southeast borderland of the Tibetan Plateau: Journal of Geophysical Research-Solid Earth, v. 110, doi: 10.1029/2004JB003421.

Tapponnier, P., Xu, Z.Q., Roger, F., Meyer, B., Arnaud, N., Wittlinger, G., and Yang, J.S., 2001, Oblique stepwise rise and growth of the Tibet plateau: Science, v. 294, p. 1671–1677, doi: 10.1126/science.105978.

Thatcher, W., 2006, Microplate model for the present-day deformation of Tibet: Journal of Geophysical Research-Solid Earth, v. 111 (in press).

Wang, Q., Zhang, P.Z., Freymueller, J.T., Bilham, R., Larson, K.M., Lai, X., You, X.Z., Niu, Z.J., Wu, J.C., Li, Y.X., Liu, J.N., Yang, Z.Q., and Chen, Q.Z., 2001, Present-day crustal deformation in China constrained by global positioning system measurements: Science, v. 294, p. 574–577, doi: 10.1126/science.1063647.

Wright, T.J., Parsons, B., England, P.C., and Fielding, E.J., 2004, InSAR observations of low slip rates on the major faults of western Tibet: Science, v. 305, p. 236–239, doi: 10.1126/science.1096388.

Zatman, S., 2000, On steady rate coupling between an elastic upper crust and a viscous interior: Geophysical Research Letters, v. 27, p. 2421–2424, doi: 10.1029/2000GL011592.

Zhang, P.Z., Shen, Z., Wang, M., Gan, W.J., Burgmann, R., and Molnar, P., 2004, Continuous deformation of the Tibetan Plateau from global positioning system data: Geology, v. 32, p. 809–812, doi: 10.1130/G20554.1.

Manuscript received 3 May 2006
Revised manuscript received 8 August 2006
Manuscript accepted 28 August 2006

Printed in USA